Ceramics International xxx (xxxx) xxx–xxx

Contents lists available at ScienceDirect

Ceramics International

journal homepage: www.elsevier.com/locate/ceramint

Role of Na-doping-induced oxygen vacancies in the variation of electrical properties of NiO ceramics

Seojin Yang[a], Jiwoong Kim[a], Sehwan Song[a], Dooyong Lee[a], Tae-Seong Ju[a], Jong-Seong Bae[b], Sungkyun Park[a,*]

[a] Department of Physics, Pusan National University, Busan 46241, Republic of Korea
[b] Busan Center, Korea Basic Science Institute, Busan 46742, Republic of Korea

ARTICLE INFO

Keywords:
$Na_xNi_{1-x}O$
Dopant
Resistivity
Oxygen vacancies

ABSTRACT

Na-doping concentration dependent electrical and structural properties of NiO ceramics were investigated. Various samples of $Na_xNi_{1-x}O$ (x = 0.00, 0.01, 0.03, 0.05, 0.07, 0.09, 0.11) were prepared by using conventional solid state reaction. Most of the samples showed the decreased electrical resistivity with the increase of the Na-doping concentration while maintaining phase-pure face-centered cubic (fcc) structure, except in the case of the sample containing 11% of Na. For the sample containing 11% of Na, the electrical resistivity slightly increased due to the presence of secondary phase. The possible physical origin of this reduced electrical resistivity is related to the increased number of oxygen vacancies, with the increase of the Na-doping concentration for phase-pure $Na_xNi_{1-x}O$ ceramics.

1. Introduction

Transparent conductive oxides (TCO) are extensively applied in various fields, such as flat panel displays [1,2], organic light emitting diodes (OLED) [3,4], solar cells [5,6] and smart windows [7,8], owing to their high transmittance in the visible range and suitable electrical conductivity [9,10]. Although Sn-doped In_2O_3 (ITO) is the most commonly used TCO materials, (e.g., SnO_2, ZnO, NiO, etc. are being studied for ITO substitution because of the rarity of Indium [11]. Among them, NiO has gained considerable attention due to its wide optical band-gap (3.6 ~ 4.0 eV) [12], chemical stability [13] and *p*-type characteristics [14–17]. However, the relatively high electrical resistivity, ρ (for example, $\rho \sim 10^{13}\ \Omega$ cm at room temperature), due to the strong electron-electron interaction in the partially filled *d*-orbital (i.e., Mott insulator), leads to difficulties in the application of potential optoelectronic devices [12,18].

Recently, several studies attempted to enhance (and/or modulate) the electrical properties of NiO. For example, Patil et al. showed that the increased electrical conductivity of NiO films with increasing annealing temperature is related to increasing grain boundaries, resulting in an increased electron scattering at the grain boundary [19]. Furthermore, Zhao et al. showed that the increase in the oxygen partial pressure during the growth of NiO films causes a decrease in the electrical resistivity and an increase in the carrier concentration [20]. Similarly, Wu et al. showed that the electrical resistivity of the NiO films decreases with the increasing of Li doping [14]. Therefore, it is believed that increasing grain size and/or doping NiO with monovalent atoms can directly influence electrical properties.

Apart from the increased electrical conductivity of NiO, the *p*-type characteristics and variation of the type of the carrier of NiO received much attention [14–17]. Recently, Denny et al. showed a similar disappearance of the *p*-type characteristics for the undoped and Na-doped NiO films, after annealing them at ~150 °C, even though they had different electrical conductivity due to Na-doping [17]. Furthermore, they mentioned the increased distortion of the neighboring oxygen atoms around the Ni atom and the presence of Ni metal vacancies as the origin of the *p*-type characteristic.

In this work, we examined the effect of oxygen vacancies in Na-doped NiO. We found the *n*-type characteristics and a decreased electrical resistivity with increasing Na-doping concentration. From core-level X-ray photoelectron spectral analysis, we found the increase of the number of oxygen vacancies with the increase of the Na-doping concentration, which explains the *n*-type characteristics and the lowering of the electrical resistivity.

2. Experiments

Na-doped NiO ($Na_xNi_{1-x}O$, x = 0.00, 0.01, 0.03, 0.05, 0.07, 0.09, 0.11) ceramics were synthesized by a solid state reaction, using an electrical muffle furnace. NiO (Sigma-Aldrich, 99%) and $NaCO_3$

* Corresponding author.
E-mail address: psk@pusan.ac.kr (S. Park).

http://dx.doi.org/10.1016/j.ceramint.2017.06.037
Received 16 May 2017; Received in revised form 5 June 2017; Accepted 6 June 2017

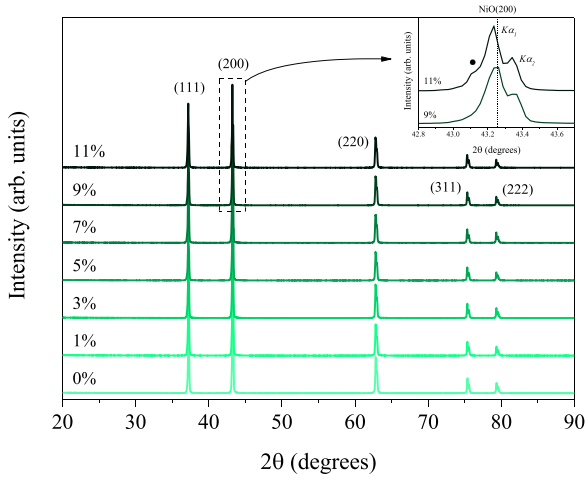

Fig. 1. X-ray diffraction patterns of Na-doped NiO powders, for various Na doping concentrations. The reference Miller indices for face-centered cubic NiO (ICSD #24018) were also listed. The inset shows the enhanced peak profiles around NiO(200); peaks for 9%- and 11%-Na-doped NiO. Owing to the Cu-anode (X-ray source), two peaks were related to Cu $K\alpha_1$ (2θ = 43.25°) and Cu $K\alpha_2$ (2θ = 43.37°) of (200) NiO (ICSD #24018). Furthermore, a shoulder peak (2θ = 43.10°) for the 11%-Na-doped NiO sample might be related to a secondary phase (i.e. (111) peak of the $NaNiO_2$ phase, ICSD #85317).

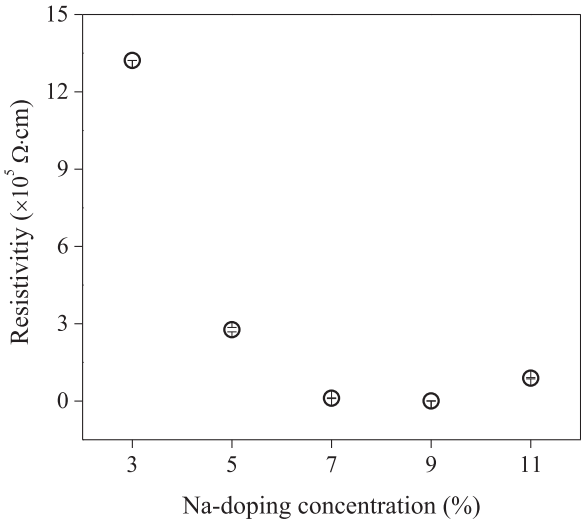

Fig. 2. Dependence of resistivity on Na-doping concentration of NiO powders. For the 0%- and 1%-Na-doped samples, the resistivity was too high to measure in the given setup.

(Sigma-Aldrich, 99.95%) powders were properly weighted and mixed, and subsequently calcined at 900 °C for 10 h in air. Then, the powders were pelletized and sintered at 1300 °C for 10 h. Structural properties of the samples were measured using X-ray diffraction (XRD, Empyrean, PANalytical) with Cu $K\alpha$ ($K\alpha_1$ = 1.5406 Å, $K\alpha_2$ = 1.5444 Å). Electrical properties were also measured by the van der Pauw method at room temperature [21–23]. The chemical state of the samples was examined using X-ray photoelectron spectroscopy (XPS, K-Alpha$^+$, Thermo Scientific) with a monochromated Al $K\alpha$ ($h\nu$ = 1486.6 eV) anode. The pass energy and step size were 50.0 eV and 0.01 eV, respectively.

3. Results and discussion

Fig. 1 shows the XRD patterns (2θ = 20–90°) of various Na-doped NiO powders. All samples showed phase-pure state, except the 11%-Na-doped NiO samples. The 11%-Na-doped NiO sample exhibited the presence of a secondary phase (see inset in Fig. 1). A detailed analysis confirmed that the secondary phase is related to a monoclinic $NaNiO_2$ structure (ICSD #85317). Furthermore, a lattice constant and unit cell volume of Na-doped NiO was calculated, by using diffraction peaks ($\theta_{(111)}$, $\theta_{(200)}$, $\theta_{(220)}$, $\theta_{(311)}$, $\theta_{(222)}$) in Fig. 1 (see Table 1). The lattice constant and unit cell volume of Na-doped NiO are larger than that of the undoped NiO. However, there were no noticeable variations of the lattice constant (or unit cell volume) depending on the doping concentration. Previously, Jang et al. [24] reported the increase of the unit cell volume with the increase of the Li-doping concentration due to the different ionic radiuses of Ni and Li (69 pm for Ni^{2+} and 76 pm for Li^+ [25]). Therefore, an appropriate substitution of Na ions into Ni-sites should increase the unit cell volume, as the ionic radius of Na (102 pm for Na^{1+}) is larger than that of Ni [25]. Park et al. calculated the increase of the unit cell volume of NiO in the presence of a Ni vacancy (or decrease in the case of oxygen) [26]. Furthermore, Chen et al. showed an increase in the lattice constant of NiO films with increasing oxygen partial pressure during film growth [27]. Therefore, it is believed that the change in the unit cell volume due to Na-doping is offset by the increase of oxygen vacancy accompanied by Na-doping.

Table 1
Na-doping-concentration-dependent lattice constants and unit cell volumes obtained from X-ray diffraction, and the electrical resistivity measured at room temperature.

Na-doping concentration (%)	Lattice constant (Å)	Unit cell volume (Å^3)	Resistivity (×10^5 Ω·cm)
0	4.1801 ± 0.0002	73.04 ± 0.08[a]	–
1	4.1810 ± 0.0002	73.19 ± 0.09	–
3	4.1813 ± 0.0002	73.10 ± 0.10	13.2159
5	4.1813 ± 0.0002	73.10 ± 0.09	2.7714
7	4.1821 ± 0.0002	73.14 ± 0.10	0.1118
9	4.1815 ± 0.0002	73.11 ± 0.10	0.0029
11	4.1826 ± 0.0002	73.17 ± 0.12	0.8876

[a] The calculated unit cell volume has no significant difference from that of the reference (73.03 Å^3, ICSD #24018).

Stoichiometric NiO is known as an insulator at room temperature but some of the NiO exhibit semiconductor characteristics, owing to nickel and/or oxygen vacancies [28]. In our study, only the NiO sample with Na doping concentration of 3–11% exhibited electrical resistivity (see Fig. 2), since the electrical resistivity of the undoped and 1%-Na-doped NiO was too high to measure. Furthermore, the electrical resistivity of NiO in the region with Na-doping concentration of 3–9% decreased with increasing doping concentration. On the other hand, for the 11%-Na-doped NiO, the electrical resistivity was higher than that of the 7%- and 9%-Na-doped NiO (see Table 1). This might be related to grain boundary scattering between the NiO and the secondary phase ($NaNiO_2$), which is also known as an insulator at room temperature [29]. From Hall effect measurement [30], all samples showed n-type characteristics with $< 10^{15}$ cm^{-3} carrier concentration, even though the specific number was not achievable, due to the large errors. It is known from previous works that the p-type characteristics of NiO is originated from Ni vacancies [14–17]. Therefore, the n-type nature of the Na-doped NiO sample is related to the presence of oxygen vacancies with Na-doping. It is worth noting that the carrier concentration of pure NiO is known to be ~10^{15} cm^{-3} [17] and it is hard to measure by using conventional measurements system.

Fig. 3 shows Na 1 s (a), Ni $2p_{3/2}$ (b) and O 1 s (c) core-level X-ray photoelectron spectra after proper calibration, with an adventitious carbon peak (284.5 eV, [31]). The vertical dotted lines indicate the reference binding energies. For Na 1 s (Fig. 4(a)), an individual peak appeared around 1071.28 ± 0.09 eV and being close to the that of Na_2SO_3 reference (1071.3 eV, [32]) suggesting the presence of a Na^{1+} state. Furthermore, the peak intensity became strong with the increase of Na-doping concentration, as expected. The quantitative analysis of the Ni $2p_{3/2}$ spectra (shown in Fig. 4(b)) is difficult, due to the complicated satellite features, caused by interatomic effects, non-local